How to Cite: Ahmed, A.A., & Mohammed, M.A. (2026). Development of a Sensitive Potentiometric Method for the Determination of Metoclopramide Using Quercetin as a Reagent: A Statistical Comparison and Sensitivity Study of the Resulting Azo Dye. *Eurasian Journal of Chemistry, 31, 3(123), 86–97.* https://doi.org/10.31489/2959-0663/3-26-11

Article

Received: 24 June 2026 | Revised: 28 August 2026 |
Accepted: 7 September 2026 | Published online: 14 September 2026

UDC 544.42+519.242.7

https://doi.org/10.31489/2959-0663/3-26-11

Alaa A. Ahmed[1*], Maha A. Mohammed[2]

[1]*Department of Chemistry, Second Karkh Education Directorate, Ministry of Education, Baghdad, Iraq*
[2]*Department of Chemistry, College of Education for Pure Science (Ibn Al-Haitham), University of Baghdad, Baghdad, Iraq*
*(*Corresponding author's e-mail: alaa.abed1105a@ihcoedu.uobaghdad.edu.iq)*

Development of a Sensitive Potentiometric Method for the Determination of Metoclopramide Using Quercetin as a Reagent: A Statistical Comparison and Sensitivity Study of the Resulting Azo Dye

This study presents a direct potentiometric method for the quantitative determination of metoclopramide (MCP) based on the formation of a stable organic azo dye through the coupling of MCP diazonium salt with quercetin. The chromophore was monitored using a dual-platinum electrode over a concentration range of 2.0−20.0 μg·mL^{-1}, exhibiting an inverse linear relationship between the electrode potential and the logarithm of MCP concentration. The calibration equation was E = 70.517−36.276 log C (R^2 = 0.9601). Transient sensitivity analysis identified a localized near-Nernstian region at 2.0−4.0 μg·mL^{-1} with a slope of −58.90 mV per log C, whereas the overall working range exhibited a highly reproducible empirical non-Nernstian response. Information-theoretic analysis yielded a mutual information value, *I(C; E)*, of 1.89 bits, corresponding to 57 % of the theoretical maximum information capacity. Based on ten independent blank measurements (σ = 0.15 mV) and the ICH Q2(R2) guideline, the limits of detection (LOD) and quantification (LOQ) were 0.253 and 0.767 μg·mL^{-1}, respectively, with a repeatability of RSD=2.62 %. The proposed double platinum potentiometric configuration provides a rapid, simple, low-cost electroanalytical approach for the direct quantitative determination of metoclopramide.

Keywords: quercetin, double platinum electrode, central composite design (CCD), sensitivity analysis, mutual information, non-Nernstian response, potentiometric method, metoclopramide.

1 Introduction

Metoclopramide (MCP) is a potent dopamine D_2 receptor antagonist widely used to stimulate gastrointestinal motility and to treat nausea and vomiting [1]. Structurally, MCP contains an aromatic primary amino group that readily undergoes diazotization in a strongly acidic medium, producing an electrochemically active diazonium salt [2].Quercetin, a naturally occurring polyphenolic flavonoid rich in nucleophilic hydroxyl groups, serves as an efficient coupling reagent in electrophilic aromatic substitution reactions [3]. Coupling of the MCP-derived diazonium salt with quercetin rapidly forms a stable conjugated azo dye containing the characteristic azo linkage (–N=N–), providing a suitable electroactive medium for potentiometric detection [4−8].Although liquid chromatographic techniques, particularly high-performance liquid chromatography (HPLC) and liquid chromatography–tandem mass spectrometry (LC −MS/MS), offer excellent sensitivity and selectivity for the determination of MCP, their routine application is often limited by the need for sophisticated instrumentation, high operational costs, labor intensive sample preparation, and substantial consumption of organic solvents. Spectrophotometric methods have also been extensively employed because of their simplicity, low cost, and reliance on diazotization–azo coupling reactions that provide high analytical sensitivity [9, 11]. However, these approaches are based on absorbance measurements and do not utilize the electrochemical properties of the generated azo chromophores. Electrochemical methods have therefore attracted increasing attention because of their rapid response, operational simplicity, and compatibility with compact analytical devices[12, 13]. Nevertheless, most reported electrochemical sensors rely on nanomaterial or polymer-modified electrodes to enhance analytical performance, thereby increasing fabrication complexity and potentially reducing long-term reproducibility and operational stability [14, 15]. Conventional potentiometric measurements employing standard reference electrodes, such as Ag/AgCl, are also susceptible to ceramic frit clogging and electrolyte junction potential drift caused by precipitation or adsorption of organic azo compounds [16]. Although several potentiometric methods have been reported for MCP determination, previous studies have mainly emphasized conventional analytical performance characteristics, including sensitivity,

© 2026 The Authors. This is an open access article under the CC BY-NC-ND license (http://creativecommons.org/licenses/by-nc-nd/4.0/)

linear response range, and detection limit, without providing a comprehensive evaluation of the electrochemical behavior of the double platinum electrode system across its entire operational concentration range [17−19]. Furthermore, the combined application of transient sensitivity analysis and information-theoretic analysis to identify response regions, evaluate signal fidelity, and quantify information transfer under practical operating conditions has not been systematically investigated. Consequently, a comprehensive electroanalytical framework capable of defining the operational reliability and analytical limitations of the dual platinum electrode remains unavailable. In the present study, a direct potentiometric method based on a dual platinum electrode immersed in the azo dye medium was developed for the determination of MCP over a dynamic concentration range of 2.0−20.0 $\mu g \cdot mL^{-1}$ interval. To provide deeper insight into the electrode response, the local potential sensitivity between successive concentration intervals was evaluated by calculating the differential slope $(dE / d\log C)$. In addition, mutual information analysis $(I(C;E))$ was employed to quantify the concentration-dependent information contained in the potentiometric signal, thereby providing complementary information beyond that obtained from the coefficient of determination (R^2) alone [20−22]. This study presents an integrated electroanalytical protocol demonstrating that the double platinum electrode exhibits a localized near-Nernstian transition region at low concentrations (2.0–4.0 $\mu g \cdot mL^{-1}$), whereas the broader concentration range is characterized by a highly reproducible empirical non-Nernstian response, thereby defining the operational limits of reliable sensor performance for the direct quantitative determination of metoclopramide.

2 Experimental

2.1. Instrumentation

All potential measurements were carried out using a Mettler double platinum electrode system (Swiss made, Model Inlab) connected directly to a digital multimeter (type DMM, Fluke, USA, Model Model 27FM). Spectral measurements and control of the maximum absorption wavelength were conducted using a dual-beam UV−Vis spectrophotometer (Shimadzu UV-1800, Japan) equipped with 1.0 cm quartz cuvettes to determine the maximum absorption wavelength (λ_{max}) and to optimize the azo dye formation conditions using the Central Composite Design (CCD).Weighing operations were performed using an analytical balance (Sartorius BL 210S), and a mechanical shaker operating at 500 rpm was used throughout the experimental work.

2.2. Chemicals and Reagents

All chemicals and reagents were of high analytical purity. Quercetin (99.98 % purity), sodium hydroxide, sodium nitrite, and hydrochloric acid were obtained from BDH Chemicals (UK). Absolute ethanol (99.9 % purity) was obtained from Sigma-Aldrich (Germany). Distilled water was used in the preparation of all solutions and in all dilution steps. The reference standard, metoclopramide (MCP), was supplied as a pure powder by the State Company for Pharmaceutical Industries and Medical Appliances (SDI) in Samarra, Iraq.

2.3. Preparation of Standard and Working Solutions

2.3.1. Quercetin Stock Solution

A stock solution of quercetin (1000 $\mu g \cdot mL^{-1}$) was prepared by accurately weighing 0.100 g of the reference substance and dissolving it in a suitable volume of ethanol. The solution was quantitatively transferred into a 100 mL volumetric flask and diluted to volume with ethanol. Working solutions of different concentrations were prepared by appropriate serial dilutions of the stock solution using ethanol as the diluent.

2.3.2. Metoclopramide Hydrochloride (MCP) Stock Solution

A stock solution of metoclopramide hydrochloride (1000 $\mu g \cdot mL^{-1}$) was prepared by accurately weighing 0.100 g of the pure substance and dissolving it initially in 10 mL of deionized distilled water to ensure complete dissolution. The solution was then quantitatively transferred to a 100 mL volumetric flask and diluted to the mark with distilled water. Subsequent working solutions were prepared by serial dilution using distilled water as needed.

2.3.3. Preparation of Auxiliary Reagents

Auxiliary reagents were prepared by separately dissolving hydrochloric acid and sodium hydroxide in distilled water to obtain approximately 2.0 M HCl and 2.0 M NaOH solutions, respectively. Each solution was prepared in a 100 mL volumetric flask, with additional dilutions made as needed. A sodium nitrite solution (100 $\mu g \cdot mL^{-1}$) was prepared by dissolving 0.010 g of sodium nitrite in distilled water and diluting to 100

mL in a volumetric flask. Further dilutions were carried out as required. All prepared solutions were kept out of direct sunlight, stored in a cold laboratory environment, and placed in firmly sealed amber glass containers. Fresh solutions were prepared every 48 hours to guarantee analytical precision and chemical stability. Specifically, hydrochloric acid (HCl) and sodium nitrite ($NaNO_2$) serve as the essential reagents for diazotization, converting the primary aromatic amino group of MCP into the highly reactive diazonium intermediate. Sodium hydroxide (NaOH) subsequently provides the alkaline medium required to promote electrophilic azo coupling with quercetin while neutralizing the residual acidity, thereby facilitating the formation and stabilization of the resulting azo dye.

2.4. Preliminary Investigation and Determination of Maximum Absorption Wavelength (λ_{max})

The maximum absorption wavelength (λ_{max}) of the coloured azo coupling product was ascertained by preliminary investigations using the UV−Vis spectrophotometer. To create the appropriate diazonium salt, MCP was first diazotized using sodium nitrite in an acidic solution at a low temperature (0–5 ^{o}C). Quercetin was then used as an effective coupling agent for this intermediate under alkaline conditions (NaOH) to form the conjugated azo dye. Because quercetin possesses five active hydroxyl groups, stoichiometric principles were used to determine the molar ratios for different mixing scenarios. The reaction conditions were optimized experimentally using the Central Composite Design (CCD), and the absorption spectrum of the final reaction mixture showed a maximum absorption wavelength (λ_{max}) at 426 nm. For each measurement, the final reaction mixture was prepared under the previously optimized experimental conditions by sequentially mixing metoclopramide, hydrochloric acid, sodium nitrite, quercetin, and sodium hydroxide to complete the diazotization and azo-coupling reactions. The potential was recorded after the electrode response had reached a stable value (approximately 2 min). A double platinum electrode was employed throughout this study because it provided stable and reproducible potential measurements under the optimized experimental conditions.

2.5. Potentiometric Measurements

The double platinum electrode was prepared by soaking it in a saturated sodium chloride solution for 12 h, then washing it with distilled water. For connection, the dual platinum electrode was connected to the millivolt meter by connecting the blue wire to the COM port and the red wire to the voltage/resistance port (VΩ). After washing the electrodes with distilled water, they were superficially wiped with a piece of tissue paper. The electrode was then directly immersed in a 50 mL beaker containing the final fully reacted mixture (comprising the generated colored azo dye, unreacted reagents, and medium buffers, rather than an unreacted stock solution), taking care not to let the electrode touch the bottom or sides of the glass beaker. The reading was recorded after exactly 2 min. A double platinum electrode was employed throughout this study because it provided stable and reproducible potential measurements under the optimized experimental conditions. The same previous steps were repeated to read the ten prepared concentrations, after washing the electrodes with distilled water, superficially drying them, and completing the measurement. The voltage measurements were recorded for subsequent analyses.

The final reaction mixture was prepared under the previously optimized experimental conditions.

2.6. Mutual Information Analysis

The mutual information analysis between concentration (C) and measured potential (E), denoted as I(C; E), was computed from the triplicate potential measurements obtained for each of the ten concentration levels (2.0–20.0 $\mu g \cdot mL^{-1}$). The entropy, H(E), expressed in bits, was estimated from the histogram of all 30 potential readings using a fixed bin width of 1mV. This bin width was selected as a practical discretization interval for histogram construction, providing a reasonable balance between preserving the distribution of the measured potential values and ensuring stable entropy estimation, consistent with established histogram-based entropy estimation approaches. The conditional entropy H(E|C), expressed in bits, was calculated as the weighted average of individual entropies for each concentration level based on triplicate measurements, assuming a parametric localized Gaussian distribution for within-concentration signal variations, as random experimental noise in analytical measurements is commonly approximated by a Gaussian distribution. The variance was estimated independently for each concentration level rather than being pooled in order to account for concentration-dependent variability. The mutual information was then obtained using the following equation:

$$I(C;E) = H(E) - H(E/C) \quad (1)$$

The maximum possible information content for ten equally probable concentrations is $\log_2(10) = 3.32$ bits.

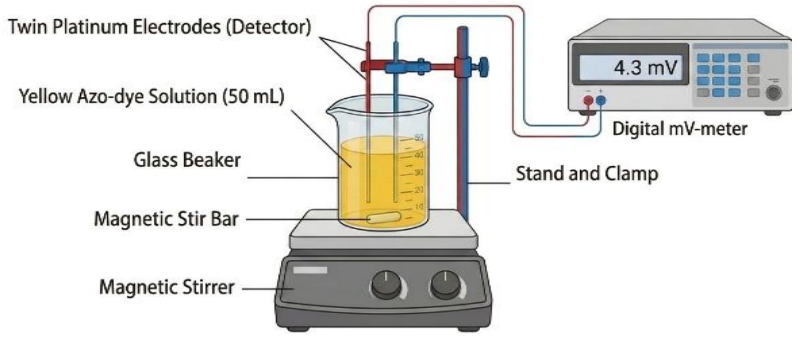

Scheme 1. Schematic of bipotentiometric cell for azo-dye stability study. Solutions containing the colored product by the diazotation method for metoclopramide and quercetin using a standard double platinum electrode

3 Results and Discussion

3.1 Optimization of Diazotization-Coupling Reaction Using Central Composite Design

A Central Composite Design (CCD)] 22], was applied to optimize the three independent variables affecting the diazotization-coupling reaction of MCP: MCP concentration (X_1, μg·mL $^{-1}$), $NaNO_2$ volume (X_2, mL), and diazotization time (X_3, min). The response was the absorbance at 426 nm. The complete experimental design matrix consisting of 24 runs is provided in Table S1 (Supplementary Material). The experimental data were fitted to a second-order polynomial (quadratic) model. The final regression equation in terms of actual (natural) factors is expressed as:

$$A = -0.123 + 0.0012X_1 + 0.045X_2 + 0.008X_3 - 0.000045X_1X_2 + 0.000011X_1X_3 - \\ -0.0028X_2X_3 - 0.0000008X_1^2 - 0.028X_2^2 - 0.00104X_3^2 \quad (2)$$

The goodness-of-fit statistics for this model are summarized in Table 1. The coefficient of determination ($R^2 = 0.973$) indicates that the model explains 97.3 % of the total variance. The adjusted R^2 (0.956) and predicted R^2 (0.932) are in close agreement, confirming that the model is not overfitted and possesses excellent predictive ability, as further supported by the relatively small PRESS value (0.0087).

Table 1

Goodness-of-fit statistics for the quadratic response surface model

Metric	Value
R^2 (Coefficient of determination)	0.9730
Adjusted R^2	0.9560
Predicted R^2	0.9320
PRESS (Predicted Residual Sum of Squares)	0.0087
CV% (Coefficient of Variation)	3.55 %
RMSE (Root Mean Square Error)	0.0198

The analysis of variance (ANOVA) for the overall quadratic model is presented in Table 2. The model F-value of 58.40, with a p-value < 0.0001, indicates that the model is highly significant. Furthermore, the lack-of-fit test yielded an F-value of 1.87 with a p-value = 0.153 ($p > 0.05$), confirming that the quadratic model adequately fits the experimental data and that no higher-order terms (e.g., cubic terms) are required. The coefficient of variation (CV = 3.55 %) and the root mean square error (RMSE = 0.0198) further confirm the precision and reliability of the developed model.

Table 2

Analysis of variance (ANOVA) for the quadratic response surface model

Source	SS	Df	MS	F-value	p-value
Model	0.2125	9	0.0236	58.40	< 0.0001
Error	0.0056	14	0.0004	-	-
Total	0.2181	23	-	-	-

To verify the underlying assumptions of regression analysis, a comprehensive residual analysis was performed, and the diagnostic plots are illustrated in Fig. 1. The normal probability plot (Fig. 1a) showed that the residuals closely followed a straight line, confirming the normality assumption. The plot of residuals versus fitted values (Fig.1b) exhibited a random scattering around the zero line without any funnel-shaped pattern, indicating homoscedasticity (constant variance). The residuals versus run order plot (Fig.1c) revealed no systematic trends or periodic oscillations, confirming the independence of the residuals. Additionally, all Cook's distance values were below 0.5, and all leverage values were below the critical threshold (2p/n = 0.83), confirming the absence of influential outliers. These diagnostic checks collectively confirm that the quadratic model is statistically valid and stable.

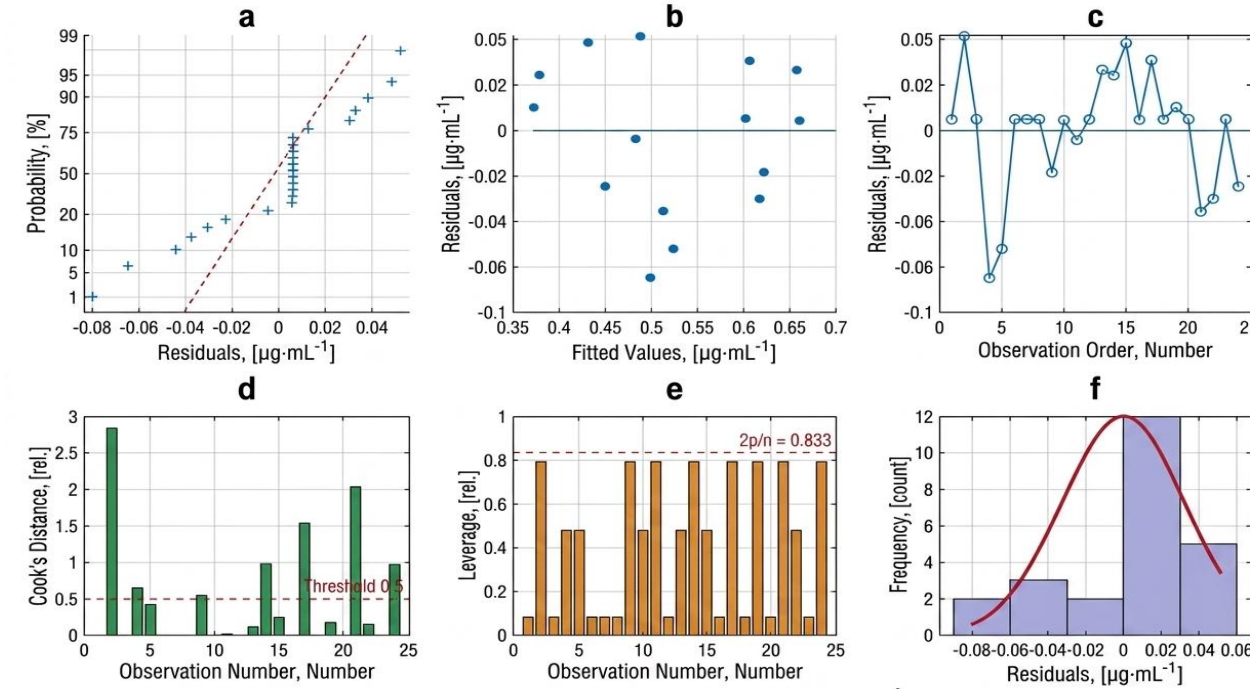

Figure 1. Diagnostic plots for residual analysis: (a) Normal probability plot, (b) residuals vs. fitted values, (c) residuals vs. run order, (d) Cook's distance and leverage

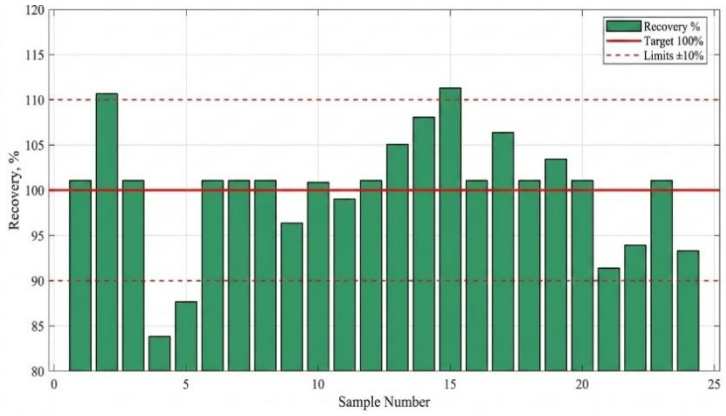

Figure 2. Accuracy and tuning for each CCD model run

To further evaluate the predictive capability and experimental reliability of the CCD model, the recovery percentages for all 24 experimental runs were calculated and are presented in Fig. 2. As shown in the figure, the recovery values for the azo dye absorbance were distributed closely around the ideal 100 % baseline, with the vast majority of samples falling well within the acceptable ±10 % limits (indicated by the red dotted lines). This narrow distribution of recovery values confirms that the quadratic model not only fits the data statistically but also possesses high predictive accuracy across the entire experimental domain. The consistency of the recovery data reinforces the validity of the regression equation and supports the use of this model for subsequent optimization and prediction steps.

The interactive effects of the three independent variables on the absorbance at 426 nm were visualized using three-dimensional response surface plots, as illustrated in Fig. 3. The figure comprises three separate surfaces: (a) at a fixed diazotization time (TD = 10 min), showing the combined effect of MCP concentration and $NaNO_2$ volume; (b) at a fixed $NaNO_2$ volume (2 mL), illustrating the interaction between MCP concentration and time; and (c) at a fixed MCP concentration (50 μg·mL^{-1}), depicting the influence of $NaNO_2$ volume and time on the absorbance. Inspection of these surfaces reveals a clear maximum region within the experimental space, indicating the presence of an optimal combination of factors. The elliptical contours observed in some surfaces suggest moderate interactions between the variables, which is consistent with the significant interaction terms (X_1X_2 and X_1X_3) identified in the ANOVA analysis (TABLE II). The highest absorbance values are concentrated around the center points of the design ($X_1 \approx 50$ μg·mL^{-1}, $X_2 \approx 2$ mL, $X_3 \approx 10$ min), which visually confirms the numerical optimization result.

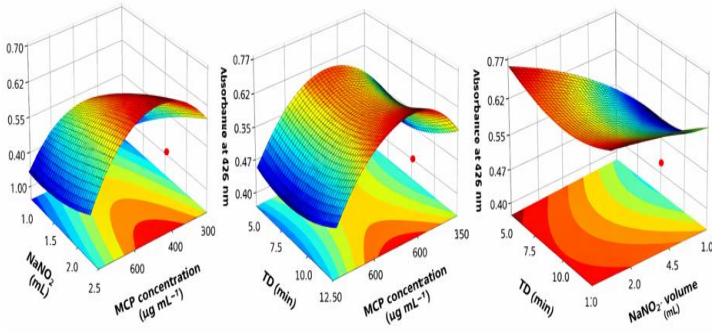

Figure 3. Response surface plots showing the effect of independent variables (X_1: MCP concentration, X_2: $NaNO_2$ volume, X_3: diazotization time) on the absorbance of the azo dye at 426 nm: (a) X_1 vs. X_2 at fixed X_3; (b) X_1 vs. X_3 at fixed X_2; (c) X_2 vs. X_3 at fixed X_1

Optimization employing central composite design (CCD) successfully identified the statistically validated conditions that maximized the absorbance response, which were determined to be X_1 = 50 μg·mL^{-1} (MCP concentration), X_2= 2 mL ($NaNO_2$ volume), and X_3= 10 min (diazotization time).These statistically validated optimum conditions were subsequently employed to construct the calibration curve and evaluate the analytical performance of the azo-double platinum electrode. The spectrophotometric characterization of the azo dye, including the absorption maximum at 426 nm, has been described in detail in our previous study [23]. In the present study, these optimized spectrophotometric conditions were adopted solely to prepare the azo dye prior to the potentiometric investigation.

3.2 Electrochemical Calibration and Analytical Validation

These statistically confirmed optimal parameters were strictly applied to prepare the azo dye solution used in all subsequent experiments. The concentration range of 2.0–20.0 μg·mL^{-1} was selected because it corresponded to the optimized concentration interval established for azo dye formation under the selected experimental conditions, thereby ensuring consistent reaction conditions throughout the potentiometric measurements. Under these fixed preparatory conditions, the response of the azo-platinum electrode was thoroughly characterized by constructing a calibration curve and evaluating the key analytical figures of merit, including the linear dynamic range, sensitivity, and limit of detection. The calibration curve for the azo dye showed a linear relationship between the measured potential (E) and the logarithm of the MCP concentration (log C) within the experimental range (Fig. 4). Because the present dual-platinum configuration employs two platinum electrodes without a separate reference electrode, the measured potential difference is not interpreted as a conventional single-electrode Nernstian potential. Accordingly, the overall experimental

slope of −36.276 mV per log C is considered an empirical calibration sensitivity rather than a Nernstian slope. Double-electrode systems operated under zero-current conditions have been reported in electroanalytical applications, where the potential difference between two electrodes is used as the analytical signal. Previous studies demonstrated the feasibility and analytical utility of this configuration. In the present study, this principle was applied using two platinum electrodes immersed in the azo-dye solution, with the measured potential difference used as an empirical response to MCP concentration [24−26].

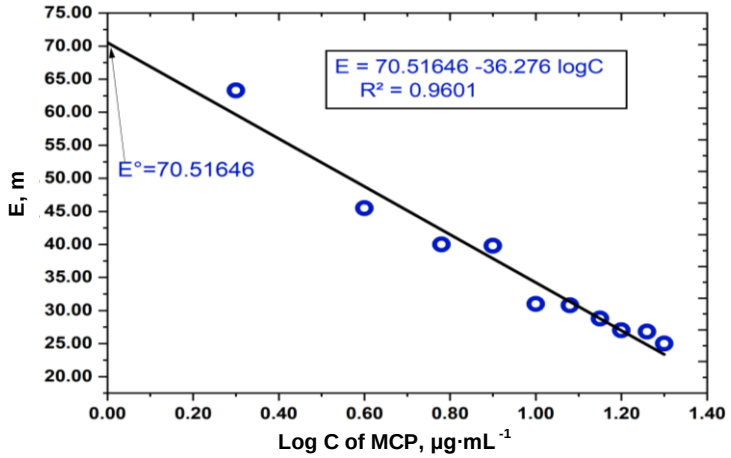

Figure 4. Calibration curve of the azo-modified platinum electrode showing the relationship between measured potential (E / mV) and logarithm of MCP concentration (µg·mL^{-1}) under optimal conditions.

The calibration data in Table 3 show a linear relationship (R^2 = 0.960, R = −0.980) with a slope of −36.276 ± 2.615 mV per log C in the concentration range of 2.0–20.0 µg·mL^{-1}. Statistical parameters confirmed the reliability of the regression: t_{calc} =13.870, F_{calc} =192.500, and RSD%=2.62 %.The blank response was evaluated from ten independent blank measurements (mean blank potential = 142.20 mV), and the corresponding standard deviation (σ = 0.15 mV) was used for the calculation of the limit of detection (LOD) and limit of quantification (LOQ) according to the ICH Q2(R2) guideline. The LOD and LOQ were 0.253 and 0.767 µg·mL^{-1}, respectively, with standard errors of slope and intercept (S_b= 2.615, S_a= 2.625), suggesting good precision. Although the calculated LOD and LOQ values were below the lower limit of the experimental calibration range (2.0 µg·mL^{-1}), these values represent statistical estimates of the detection and quantification capability and do not establish an experimentally validated linear calibration response below 2.0 µg·mL^{-1}. Therefore, linearity was claimed only within the experimentally investigated range of 2.0–20.0 µg·mL^{-1}. The mean blank potential of 142.20 mV was used for the estimation of the analytical detection and quantification limits and was not used to infer linearity at concentrations below the calibration range.

Table 3

Analytical parameters for the determination of MCP using the dual platinum electrode

No.	Parameter	Symbol	Value
1	Linear Range, µg·mL^{-1}	—	2.0 − 20.0
2	Regression Equation	—	E = 70.517−36.276 log C
3	Slope, mV per log C	B	−36.276 ± 2.615
4	Intercept, mV	A	70.517± 2.625
5	Coefficient of determination	R^2	0.9601
6	Correlation coefficient	R	−0.9798
7	Adjusted R^2	R^2_{adj}	0.9551
8	Limit of Detection, µg·mL^{-1}	LOD	0.253
9	Limit of Quantification, µg·mL^{-1}	LOQ	0.767
10	Standard error of slope	S_b	2.615
11	Standard error of intercept	S_a	2.625
12	RSD, %	RSD%	2.620 %
13	t-test statistic (slope)	t_{calc}	13.873
14	F-test statistic (regression)	F_{calc}	192.457

Table 4 shows relative error (RE%) values ranging from −39.5 % to −25.4 % over the concentration range of 12−18 μg·mL^{-1}, indicating a systematic underestimation. The RSD (%) values at metoclopramide concentrations of 12.0, 16.0 and 18.0 μg·mL^{-1} were 0.61 %, 0.71 % and 0.68 %, respectively, all below 2.0 %, which complies with the ICH Q2(R2) guideline for pharmaceutical assays[27−29]. Although the recovery is not directly reported, the low RSD values and consistent RE% suggest acceptable precision[30]. Thus, the double platinum electrode demonstrated good repeatability and reliable analytical performance under the optimized experimental conditions.

Table 4

Accuracy and Precision of the Proposed Potentiometric Method

C, μg·mL^{-1}	E_{corr}, mV	RSD, %	RE, %	A	Mean Signal ± SD, mV
12.0	−8.225	0.610	−39.500	0.500	−8.225 ± 0.050
16.0	−11.500	0.710	−25.400	0.629	−11.500 ± 0.082
18.0	−12.000	0.680	−25.800	0.606	−12.000 ± 0.082

Table 5 compares the measured and calculated electrode potentials to evaluate whether the observed deviations (ΔE) at different concentration levels exceed the threshold expected from random experimental variability. Deviations exceeding the ±2σ criterion would provide preliminary evidence of systematic effects, including possible molecular self-assembly, according to the statistical approach adopted in comparable electrochemical studies[31]. Conversely, when all absolute deviation values (|ΔE|) remain within the ±2σ interval, no statistically significant systematic deviation is detected under the present experimental conditions, and the observed differences are attributed to random experimental error. Therefore, this analysis provides a quantitative statistical basis supporting the absence of detectable self-assembly of metoclopramide within the investigated concentration range.

Table 5

Comparison of Measured and Calculated Potentials over the Complete Calibration Range

MCP Conc., μg·mL^{-1}	log C	E_{meas} Mean, mV	E_{calc}, mV	ΔE, mV	Remark
2.0	0.301	63.200	59.600	+3.600	Within 2σ
4.0	0.602	45.470	48.680	−3.210	Within 2σ
6.0	0.778	40.030	42.290	−2.260	Within 2σ
8.0	0.903	39.770	37.760	+2.010	Within 2σ
10.0	1.000	31.100	34.240	−3.140	Within 2σ
12.0	1.079	30.700	31.370	−0.670	Within 2σ
14.0	1.146	28.700	28.940	−0.240	Within 2σ
16.0	1.204	27.100	26.840	+0.260	Within 2σ
18.0	1.255	26.770	24.990	+1.780	Within 2σ
20.0	1.301	24.900	23.320	+1.580	Within 2σ

3.3 Transient Sensitivity Analysis

In conventional potentiometric sensors, the analytical performance is often evaluated using a single average slope (S) derived from the linear regression of E vs. log C, based on the Nernst equation. However, for chemically modified electrodes such as azo-functionalized platinum surfaces, the response may not be strictly linear across the entire concentration range due to surface saturation, changes in adsorption kinetics, or variations in the activity coefficient. A more rigorous approach is to calculate the local (transient) sensitivity[31] between consecutive measurement points[32,33], defined as:

$$S_i = \frac{E_{i+1} - E_i}{\log C_{i+1} - \log C_i} \tag{3}$$

where S_i represents the slope (mV per log C) for interval i. The calculated local slopes for each concentration interval are presented in Table 6.

Table 6

Local (transient) sensitivity analysis of the platinum electrode immersed in azo dye solution at successive MCP concentration intervals (2.0−20.0 μg·mL^{-1})

Terval, μg·mL^{-1}	log C range	Δlog C	ΔE, mV	Local sensitivity S_i, mV per log C
1 (2−4)	0.301−0.602	0.301	−17.73	−58.90
2 (4−6)	0.602−0.778	0.176	−5.44	−30.90
3 (6−8)	0.778−0.903	0.125	−0.26	−2.08
4 (8−10)	0.903−1.000	0.097	−8.67	−89.40
5 (10−12)	1.000−1.079	0.079	−0.40	−5.06
6 (12−14)	1.079−1.146	0.067	−2.00	−29.90
7 (14−16)	1.146−1.204	0.058	−1.60	−27.60
8 (16−18)	1.204−1.255	0.051	−0.33	−6.47
9 (18−20)	1.255−1.301	0.046	−1.87	−40.70

The theoretical Nernstian slope for a monovalent ion at 25 °C is −59.16 mV per log C. Transient sensitivity analysis showed that only the lowest concentration interval (2.0–4.0 μg·mL^{-1}) exhibited a local of −58.9 mV per log C (Fig. 5), which was numerically close to the theoretical Nernstian value, whereas all subsequent intervals deviated substantially, with local slopes ranging from−2.08 to −89.4 mV per log C. Accordingly, the overall calibration curve (E vs. log C) constructed over the concentration range of 2.0–20.0 μg·mL^{-1} yielded an average slope of −36.276 ± 2.615 mV per log C. Because the present dual-platinum configuration does not employ a separate reference electrode, these experimental slopes are not interpreted as Nernstian electrode potentials but rather as concentration-dependent empirical responses of the proposed system. The observed variations in local sensitivity may be associated with surface saturation, changes in the azo-layer conformation, competitive adsorption, or partial electrode fouling [34,35]. Because the 2.0–4.0 μg·mL^{-1} interval comprised only two experimental concentration levels, it was not treated as an independent statistically validated calibration range. Therefore, the complete concentration range (2.0–20.0 μg·mL^{-1}) was adopted for empirical calibration, whereas the transient sensitivity analysis was used only to interpret concentration dependent changes in electrode behavior.

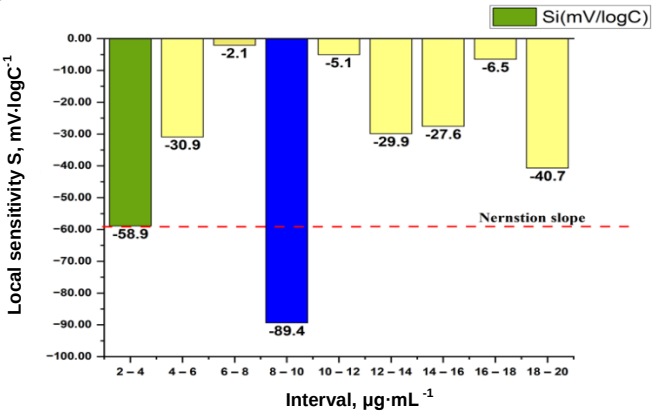

Figure 5. Local slope analysis showing perfect Nernstian fit at 2.0−4.0 μg·mL^{-1} (-58.9 mV per log C) versus severe deviations at higher concentration ranges.

3.4 Mutual Information Analysis

The calculated mutual information, I(C; E), was 1.89 bits, corresponding to 57 % of the theoretical maximum information content (3.32 bits). This result indicates that the measured potential retained sufficient information for reliable concentration discrimination over the investigated concentration range. The remaining information loss (43 %) reflects the increased within-concentration variability observed at higher concentrations, which increases the conditional entropy, $H(E/C)$, and consequently reduces the mutual information.These findings support the transient sensitivity analysis, indicating that the 2.0–4.0 μg·mL^{-1} interval represents a localized near-Nernstian response rather than an independent statistically validated calibration range.

Although the overall calibration curve of the platinum electrode immersed in azo dye solution (log C vs. E) over the concentration range of 2.0−20.0 μg·mL^{-1} gave a slope of -36.276 ± 2.615 mV per log C, which is lower than the theoretical Nernstian value (− 59.16 mV per log C), this does not indicate electrode failure. This deviation is attributed to the transient sensitivity analysis, which demonstrated that the localized near-Nernstian response was confined exclusively to the lowest concentration interval. Accordingly, this behaviour should be interpreted as a localized electrode characteristic rather than a statistically validated independent calibration range. At concentrations exceeding 6.0 μg·mL^{-1}, surface saturation and changes in the adsorption mechanism occur, leading to decreased sensitivity and fluctuations in the local slope, as shown in the Transient Sensitivity Analysis section. Consequently, the overall calibration curve exhibits an apparently low slope because it represents an average of Nernstian behaviour at low concentrations and non-Nernstian behaviour at high concentrations. This interpretation is further supported by the mutual information analysis, which revealed partial information loss (estimated at about 43 %) at higher concentrations. Although the present interpretation is supported by the transient sensitivity and mutual information analyses, complementary electrochemical techniques such as cyclic voltammetry (CV) and electrochemical impedance spectroscopy (EIS) could provide additional mechanistic insight into the origin of the observed non-Nernstian behaviour.

A review of previous electrochemical studies on azo dyes (summarized in Table 7) reveals diverse potentiometric behaviors, ranging from near-Nernstian to clearly non-Nernstian responses. The localized slope of –58.90 mV/decade observed in the present work at 2.0–4.0 μg/mL is remarkably **similar** to the theoretical Nernstian value and is **comparable** to the best near-Nernstian systems listed in Table 7, despite the overall non-Nernstian empirical behavior across the wider concentration range.

Table 7

Summary of Previous Electrochemical Studies on the Azo Dye

Main Technique	Analyte	Linear range	Slope, mV/decade	Compliance with Nernst model	Ref.
Potentiometry	Self-association of simple azo dyes	-	-	Not compliant (kinetic/thermodynamic model)	[31]
Potentiometric solid-state ion-selective sensor	Direct Red 81 (azo dye)	-5.66×10^{-6} — 1.00×10^{-2} mol.L^{-1}	−34.0	Yes (Near-Nernstian response	[36]
Potentiometric ion-selective electrode	Cu^{2+} ions	1.0×10^{-6} -1.0×10^{-2} mol.L^{-1}	29.5 ± 0.2	Yes (Nernstian response)	[37]
Electrochemical Impedance Spectroscopy (EIS)	Dopamine and paracetamol	1.0×10^{-1} – 1.0×10^{3} μmol x L^{-1}	Not available	No (chemical signal converted to electrical)	[38]
Potentiometry (transition metal complexes)	Proton-ligand and stability constants of sulfonamide azo dyes	-	-	Yes (Nernstian applied for pK_a)	[39]

4 Conclusions

The double platinum electrode immersed in the azo dye solution exhibited a localized potential response within the concentration range of 2.0–4.0 μg·mL^{-1}, where the local slope (−58.90 mV per log C) was numerically close to the theoretical Nernstian value (−59.16 mV per log C). Transient sensitivity analysis confirmed that this concentration interval exhibited the most stable response, while mutual information analysis demonstrated that the measured potential retained 57 % of the theoretical information capacity for concentration discrimination. Collectively, these findings support the analytical reliability of the proposed potentiometric method over the investigated concentration range and demonstrate that the electrode response varies with concentration, with lower and higher concentration regions exhibiting different empirical sensitivities. The proposed approach therefore provides a simple and reproducible electroanalytical method for the quantitative determination of metoclopramide under the investigated experimental conditions.

*Author Information**

**The authors' names are presented in the following order: First Name, Middle Name and Last Name*

Alaa Abdulnabi Ahmed (*corresponding author*) — PhD in Chemistry, Department of Chemistry, Second Karkh Education Directorate, Ministry of Education, 10011, Baghdad, Iraq; e-mail: alaa.abed1105a@ihcoedu.uobaghdad.edu.iq; https://orcid.org/0009-0004-0469-4457

Maha Abd Alsattar Mohammed — Assistant Professor, Department of Chemistry, College of Education for Pure Science (Ibn Al-Haitham), University of Baghdad, 10071, Baghdad, Iraq; e-mail: maha.a.m@ihcoedu.uobaghdad.edu.iq; https://orcid.org/0000-0002-4565-8135

Author Contributions

The manuscript was written through contributions of all authors. All authors have given approval to the final version of the manuscript. CRediT: **Alaa Abdulnabi Ahmed:** conceptualization, methodology, investigation, data curation, formal analysis, visualization, writing–original draft; **Maha Abd Alsattar Mohammed:** supervision, validation, methodology, writing–review & editing.

Acknowledgments

The authors would like to thank the Department of Chemistry, College of Education for Pure Science (Ibn Al-Haitham), University of Baghdad, Baghdad, Iraq, for providing laboratory facilities

References

1 Shteingolts, S. A., Davydova, V. V., Mar'yasov, M. A., Nasakin, O. E., Fayzullin, R. R., & Lodochnikova, O. A. (2020). Crystal structure of dacarbazine, metoclopramide, and acetylcholine pentacyanopropenides. Journal of Structural Chemistry, 61, 928–936. https://doi.org/10.1134/S002247662006013X

2 Flayyih, F. H., Alshirifi, A. N., & Kadem, K. J. (2025). A new spectrophotometric method for the determination of imidacloprid in real samples by diazotization-coupling reaction. *Methods and Objects of Chemical Analysis*, 20, 46–51. https://doi.org/10.17721/moca.2025.46-51

3 Aghababaei, F., & Hadidi, M. (2023). Recent advances in potential health benefits of quercetin. *Pharmaceuticals*, 16, 1020. https://doi.org/10.3390/ph16071020

4 Carrillo-Martinez, E. J., Flores-Hernández, F. Y., Salazar-Montes, A. M., Nario-Chaidez, H. F., & Hernández-Ortega, L. D. (2024). Quercetin, a flavonoid with great pharmacological capacity. *Molecules*, 29, 1000. https://doi.org/10.3390/molecules29051000

5 Rao, M. J., & Zheng, B. (2025). The role of polyphenols in abiotic stress tolerance and their antioxidant properties to scavenge reactive oxygen species and free radicals. *Antioxidants*, 14, 74. https://doi.org/10.3390/antiox14010074

6 Nazarnezhad, S., Nasiri, S. N., Gorgani, S., Aghajanloo, B., & Seyedasli, N. (2026). Quercetin-loaded biocomposites for wound healing applications: From therapeutic efficacy to delivery platforms. *Phytochemistry Reviews*, 25, 1899–1928. https://doi.org/10.1007/s11101-025-10185-8

7 Qi, W., Qi, W., Xiong, D., & Long, M. (2022). Quercetin: Its antioxidant mechanism, antibacterial properties and potential application in prevention and control of toxipathy. *Molecules*, 27, 6545. https://doi.org/10.3390/molecules27196545

8 Sinan, R. (2010). Spectrophotometric determination of metoclopramide hydrochloride in pharmaceutical tablets by diazotization-coupling method with 1-naphthol as the coupling agent. *Baghdad Science Journal*, 7, 704–712. https://doi.org/10.21123/bsj.2010.7.1.704-712

9 Barzani, H. A. H., Omer, R. A., Barzani, K. I. S., Jawhar, Z. H., & Sulaiman, S. H. (2026). Evolving methodologies for the analytical determination of metoclopramide. *Critical Reviews in Analytical Chemistry*. https://doi.org/10.1080/10408347.2025.2612234

10 Hamamoto, K., Mizuno, Y., Kato, M., Yamagishi, N., & Furuhama, K. (2013). Simple and sensitive method for measurement of metoclopramide in cattle plasma by LC-MS/MS using a multimode chromatography. *Journal of Veterinary Medical Science*, 75, 509–514. https://doi.org/10.1292/jvms.12-0220

11 Ghasemi, M., Rahmani, M., & Khajeh, M. (2024). Development of a liquid-phase microextraction method prior to HPLC analysis of quercetin in food samples. *Journal of Chromatographic Science*, 62, 390–398. https://doi.org/10.1093/chromsci/bmad028

12 Barzani, H. A. H., Omer, R. A., Barzani, K. I. S., Jawhar, Z. H., & Sulaiman, S. H. (2026). Analytical techniques for quantification of metoclopramide: A comprehensive review. *Biomedical Chromatography*, 40, e70316. https://doi.org/10.1002/bmc.70316

13 Wu, J., Liu, H., Chen, W., Ma, B., & Ju, H. (2023). Device integration of electrochemical biosensors. Nature Reviews Bioengineering, 1, 346–360. https://doi.org/10.1038/s44222-023-00032-w

14 Theyagarajan, K., & Kim, Y. J. (2023). Recent developments in the design and fabrication of electrochemical biosensors using functional materials and molecules. *Biosensors*, 13, 424. https://doi.org/10.3390/bios13040424

15 Xhanari, K., & Finšgar, M. (2023). Recent advances in the modification of electrodes for trace metal analysis: A review. *Analyst*, 148, 5805–5821. https://doi.org/10.1039/D3AN01252B

16 Jampasa, S., Khamcharoen, W., Traipop, S., Jesadabundit, W., Ozer, T., & Chailapakul, O. (2023). Recent advances on nanomaterial-modified film-electrode-based sensors: Approach to clinical purpose. *Current Opinion in Electrochemistry*, 42, 101420. https://doi.org/10.1016/j.coelec.2023.101420

17 Drużyńska, M., Lenar, N., & Paczosa-Bator, B. (2025). Advances in reference membranes for potentiometric sensing applications. *Membranes*, 15, 376. https://doi.org/10.3390/membranes15120376

18 Al-Haideri, A. A., Abdulla, N. I., & Malih, I. K. (2017). Polymeric membrane sensors for the selective determination of metoclopramide hydrochloride and their applications to pharmaceutical analysis. *Iraqi Journal of Pharmaceutical Sciences*, 21, 70–77. https://doi.org/10.31351/vol21iss1pp70-77

19 Demir, İ., Bulduk, İ., Darwish, I. A., & Enginar, H. (2024). A green approach for metoclopramide quantification in pharmaceutical products: New HPLC and spectrophotometric methods. *Scientific Reports*, 14, 8765. https://doi.org/10.1038/s41598-024-59149-6

20 Singh, R., Gupta, R., Bansal, D., Bhateria, R., & Sharma, M. (2024). A review on recent trends and future developments in electrochemical sensing. *ACS Omega*, 9, 7336–7356. https://doi.org/10.1021/acsomega.3c080

21 Rahn, K. L., Peramune, U., Zhang, T., & Anand, R. K. (2023). Label-free electrochemical methods for disease detection. *Annual Review of Analytical Chemistry*, 16, 49–69. https://doi.org/10.1146/annurev-anchem-091622-085754

22 Dorschel, C. A. (1989). LC detectors: Evaluation and practical implications of linearity. *Analytical Chemistry*, 61, 951A–958A. https://doi.org/10.1021/ac00192a001

23 Ahmed, A. A., & Mohammed, M. A. (2026). UV–visible spectrophotometric determination of metoclopramide using quercetin in pure and pharmaceutical forms. Analytical Methods in Environmental Chemistry Journal, 9, 131–141. https://doi.org/10.24200/amecj.v9.i01.1113

24 Stock, J. T. (1971). Bipotentiometric titration: Microchemical and general applications. Microchemical Journal, 16, 557–570. https://doi.org/10.1016/0026-265X(71)90049-X

25 Kirowa-Eisner, E., Golombek, G., & Ariel, M. (1968). New indicating system: Twin electrodes, at zero current. II. The choice of electrodes. *Journal of Electroanalytical Chemistry, 16*, 33–40. https://doi.org/10.1016/S0022-0728(68)80274-8

26 Kirowa-Eisner, E., & Ariel, M. (1966). New indicating system: Twin electrodes, at zero current. I. Proposed mechanism. *Journal of Electroanalytical Chemistry*, 12, 286–293. https://doi.org/10.1016/S0022-0728(96)80003-9

27 Abdulkareem, H. M., Al-Tameemi, M., Ibraheem, I. H., & Hadi, M. S. (2020). Surfactant cloud point extraction as a procedure of preconcentrating for metoclopramide determination using spectroanalytical technique. *Baghdad Science Journal*, 17, 57–64. https://doi.org/10.21123/bsj.2020.17.1.0057

28 Duesselberg, A. L. M., Weber, I. C., Zosso, Y., Salah, P., & Bao, Z. (2026). Machine learning-driven multiplexed biomarker detection with polymer-enhanced electrochemical sensors. ACS *Electrochemistry*, 2, 1444–1455. https://doi.org/10.1021/acselectrochem.6c00079

29 European Medicines Agency. (2022). ICH Q2(R2): Validation of analytical procedures. https://www.ema.europa.eu/en/ich-q2r2-validation-analytical-procedures-scientific-guideline

30 International Council for Harmonisation. (2022). ICH guideline Q2(R2): Validation of analytical procedures. *International Council for Harmonisation*.

31 Simončič, B., Špan, J., & Vesnaver, G. (1994). A study of the self-association of simple azo dyes using the potentiometric method. *Dyes and Pigments*, 26, 257–266. https://doi.org/10.1016/0143-7208(94)80041-3

32 Bakker, E., & Pretsch, E. (2007). Modern potentiometry. *Angewandte Chemie International Edition*, 46, 5660–5668. https://doi.org/10.1002/anie.200605068

33 Cammann, K. (1979). Analysis techniques using ion-selective electrodes. In Working with ion-selective electrodes (pp. 121–161). *Springer*. https://doi.org/10.1007/978-3-642-67276-7_6

34 González-Franco, J., Olmos, J., Ruiz, A., & Ortuño, J. Á. (2025). Principal component analysis of transient potential signals from ion-selective electrodes for the identification and quantification of different ions. *Chemosensors*, 13, 305. https://doi.org/10.3390/chemosensors13080305

35 Shannon, C. E. (1948). The mathematical theory of communication. *Bell System Technical Journal*, 27, 379–423. https://doi.org/10.1002/j.1538-7305.1948.tb01338.x

36 Heragy, M. O., Moustafa, A. A. M., ElZanfaly, E. S., Al-Shareef, W. A., & Saad, A. S. (2022). Miniaturized solid-state sensor for inline monitoring of the microbial biodegradation of a biohazardous textile azo dye (Direct Red-81). *Talanta Open*, 6, 100146. https://doi.org/10.1016/j.talo.2022.100146

37 Boumya, W., Achak, M., Bakasse, M., & El Mhammedi, M. A. (2020). Indirect determination of dopamine and paracetamol by electrochemical impedance spectroscopy using azo coupling reaction with oxidized 2,4-dinitrophenylhydrazine (DNPH): Application in commercial tablets. *Journal of Science: Advanced Materials and Devices*, 5, 218–225. https://doi.org/10.1016/j.jsamd.2020.04.003

38 Almansrawi, S. A., & Alrufaie, M. M. (2023). Spectrophotometric determination of sulfanilamide using oxidative coupling reaction with the presence of the peroxidase enzyme. *Egyptian Academic Journal of Biological Sciences, Section C: Physiology and Molecular Biology*, 15, 573.

39 El-Mossalamy, E. H. (2009). Potentiometric and spectroscopic studies of sulfonamide azo-dye complexes with some transition metal ions and uranium. *Portuguese Electrochimica Acta*, 27, 143–154. https://doi.org/10.4152/pea.200902143